ULUSLARARASI 3B YAZICI TEKNOLOJİLERİ
VE DİJİTAL ENDÜSTRİ DERGİSİ

INTERNATIONAL JOURNAL OF 3D PRINTING
TECHNOLOGIES AND DIGITAL INDUSTRY

ISSN:2602-3350 (Online)

URL: https://dergipark.org.tr/ij3dptdi

NUMERICAL AND EXPERIMENTAL INVESTIGATION OF THE EFFECT OF DELAMINATION DEFECT AT MATERIALS OF POLYETHYLENE TEREPHTHALATE (PET)PRODUCED BY ADDITIVE MANUFACTURING ON FLEXURAL RESISTANCE

Yazarlar (Authors): Alperen Dogru, Ayberk Sozen*, Gokdeniz Neser, M. Ozgur Seydibeyoglu

Bu makaleye şu şekilde atıfta bulunabilirsiniz (To cite to this article): *Dogru A.,* Sozen *A., Neser G.,* Seydibeyoglu *M. O., "Numerical and Experimental Investigatiqon of The Effect of Delamination Defect at Materials of Polyethylene Terephthalate (Pet)Produced By Additive Manufacturing on Flexural Resistance" Int. J. of 3D Printing Tech. Dig. Ind., 6(3): 382-391, (2022).*

DOI: 10.46519/ij3dptdi.1098903

Araştırma Makale/ Research Article

Erişim Linki: (To link to this article): https://dergipark.org.tr/en/pub/ij3dptdi/archive

NUMERICAL AND EXPERIMENTAL INVESTIGATION OF THE EFFECT OF DELAMINATION DEFECT AT MATERIALS OF POLYETHYLENE TEREPHTHALATE (PET)PRODUCED BY ADDITIVE MANUFACTURING ON FLEXURAL RESISTANCE

Alperen Dogru[a,b], Ayberk Sozen[c]*, Gokdeniz Neser[c], M. Ozgur Seydibeyoglu[d,e]

[a] Ege University, Aviation HVS, Aircraft Technology, TURKEY
[b] University of Alberta, Mechanical Engineering, CANADA
[c] Dokuz Eylul University, Institute of Marine Sciences and Technology, TURKEY
[d] İzmir Katip Çelebi University, Material Sciences, and Engineering, TURKEY
[e] Maine University, Advanced Structures & Composites Center, USA
* *Corresponding Author: ayberk.sozen@deu.edu.tr*

(**Received:** 05.04.2022; **Revised:** 30.09.2022; **Accepted:** 10.11.2022)

ABSTRACT

Polyethylene terephthalate (PET) material, universally used in the packaging industry due to its thermal and mechanical properties, high chemical resistance, and low gas permeability, is among the most widely used polymer materials worldwide. These properties have made their use in additive manufacturing methods widespread. Determining how some common additive manufacturing defects affect the products produced by these methods will increase the adoption of these technologies in final production. In this study, the effect of layer non-joining defect called delamination on the impact strength of PET material produced by additive manufacturing method at different layer thicknesses was carried out experimentally and numerically. The effects of flexural stress on the artificially created layer adhesion defect on the middle layers of the parts produced and modelled with a layer thickness of 0.1/0.2/0.3 mm were investigated. It has been discovered that the increase in layer thickness decreases flexural strength. In addition, while the flexural strength of the specimens containing delamination decreased, the growth in layer thickness accelerated this decrease.

Keywords: PET, Flexural Resistance, Delamination, FFF.

1. INTRODUCTION

The increase in the variety of materials used in additive manufacturing methods and the determination of the mechanical behaviour of the parts produced by this method ensure widespread use in creating final pieces. Additive manufacturing methods, which were previously used in the production of pre-trial parts, allow usage in many different fields thanks to the developments in equipment technologies and advances in materials science [1]. Additive manufacturing has an increasing share among the production methods of polymer materials. Exconde et al. [2], reported that producing environmentally-friendly polymer materials with these methods is essential for a sustainable world, studies on this subject are critical.

The packaging industry is an important constituent of trade around the world. Packaging wastes constitute the most crucial part of the plastic waste problem [3]. In addition, the growing demand for plastic products in the packaging industry makes this situation even worse [4]. Polyethylene terephthalate (PET) material finds widespread application in food and beverage packaging due to its superb thermal and mechanical properties, high chemical endurance, and low gas permeability [5,6]. In addition, PET is a versatile polymer in films, blow-moulded, and injection-moulded products [7]. PET does not pose a direct danger to the environment. However, its high usage volume creates a large amount of waste and is resistant to degradation [8]. PET melts between 255 and 265°C, while PET materials with higher crystallinity melt at higher temperatures [9]. PET's tendency to

crystallise reduces its transparency [10]. PET material has good forming performance, high impact strength, tensile toughness, transparency, and chemical resistance [11]. PET material, a thermoplastic polymer, is widely used as a consumable in the manufacture of bottles, containers, and packaging materials for various food and medical products and commercial applications due to its properties [7].

The ability of PET to be shaped at low temperatures has made it a desirable material for additive manufacturing methods [12]. Thermoplastic polymer materials and polymeric matrix composites can be processed in the Fused Filament Fabrication (FFF) method, which slices the geometry of the part to be produced in layers and creates parts by extruding the material in the cartesian system. In this method, also called 3D printing, polymeric filaments are produced by extrusion [2]. Many different parameters are used in making parts with the FFF method [13]. Namely, nozzle temperature, layer thickness, infill per cent, infill pattern, print speed, material flow, etc. There are many studies on PET and PETG materials production in the FFF method. Various experimental studies have been carried out to analyse the effect of process parameters such as layer thickness, infill per cent, and infill pattern on mechanical properties.

Kumar et al. [12], examined the specimens produced from PETG material by the FFF method. The samples were produced at different printing speeds, infill per cent, and layer thicknesses. Production parameters are optimised with the results of tensile, bending, and hardness tests.

Srinivasan et al., [14], in their study, stated that among the FFF process parameters, the tensile strength decreased with the increase of layer thickness, and the tensile strength increased with the rise of the infill per cent. In addition, they observed that the filling pattern combined with the structure's orientation created differences in the tensile strength and determined that the surface roughness value decreased with the increase of the infill per cent.

Durgashyam et al. [15], investigated the effect of print speed, infill per cent, and layer thickness on the processing of PETG material in the FFF method. They concluded that PETG material exhibited good mechanical properties at lower layer thickness. These studies guide the parameters to be used in the production of PET/PETG products with FFF. Szczepanik et al. [1], investigated the bending and compression mechanical properties of PET and Acrylonitrile Butadiene Styrene (ABS) specimens produced as circular and rectangular patterns with a 3D printer. Sepahi et al. [16], compared the mechanical properties of PETG specimens produced by the FFF method with PLA and ABS specimens While PETG material has the similar tensile strength to PLA and ABS, it has been determined that its ductility is higher. Hanon et al. [17], investigated the mechanical properties of tensile test specimens produced by the FFF 3D printing method using PETG materials. They examined the effects of raster direction angles, print orientations, and infill percentage and patterns to investigate the impact on anisotropy in specimens produced with FFF. The highest tensile strength and elongation values were measured in the 0° raster direction and the Y orientation. In addition, PLA and PETG specimens were compared. A comparison between PETG and PLA showed that PETG gave better elongation results. They experienced that PETG gave better elongation results. Mansour et al. [18], investigated the mechanical and dynamic behaviour of PETG produced by the FFF method and PETG reinforced with 20% carbon fibre. As a result, it is revealed that adding carbon fiber reduces the compression stress by 66% and increases the modulus and stiffness by 30% and 27%, respectively. Exconde et al. [2], compared FFF-produced specimens of pure PET and recycled PET materials. They compared the melting point and MFI values. They have observed that recycled PET is more flexible and easier to process. This has shown that recycled PET will be re-filamented for use in the FFF method and even show better processability.

All studies compare the mechanical properties of PET/PETG specimens produced with different parameters in the FFF method and examine the effect of recycling and fibre reinforcement.

There are also various studies on the numerical analysis of specimens produced by the FFF method. Fonseca et al. [19], performed the fracture toughness analysis of PA12 samples produced by the FFF method and PA12 models

with carbon fibre reinforcement numerically and experimentally.

Atlıhan et al. [20], investigated the effect of natural frequency values on beam structures with honeycomb geometry produced from PLA material by the FFF method. Numerical and experimental analyses of the directed beams were carried out. Somireddy et al. [21], investigated the role of mesostructured aspects on the general mechanical properties of the parts produced by the FFF method. In particular, the effects of fibre orientation, layer thickness, and lamina placement on the properties of the manufactured parts were investigated numerically.

Critical methodologies that will contribute to the literature have been revealed in these studies, where different polymers are discussed.

Yao et al. [22], investigated the elastic properties of the parts produced with FFF and the vibration properties of these specimens. Tensile samples with nine different compression directions and three different layer thicknesses were made to create the orthotropic elastic structural relationship. Also, based on this relationship, numerical models are constructed to simulate vibration properties in a plate produced with FFF. The methodologies put forward in modelling experimental studies in additive manufacturing technology in a computer environment are critical and give direction to this field.

Problems frequently encountered in the FFF method, the most widely used polymer production among additive manufacturing methods, cause defective productions [23,24]. Nozzle clogging, non-adhesion of the first layer, incomplete extruding of the material, deformation (warping) of the part in the production, failure of the layers to coalesce (delamination), etc are some of the defects. It is known that the parts produced by the FFF method exhibit anisotropic properties [17]. The axis in which the parts made with FFF exhibit the lowest mechanical properties is the z-axis [25,26]. Because the part is extruded in layers due to the nature of the manufacturing technology, the layers must bond together and strengthen in the z-direction. Parameters such as choosing the appropriate nozzle temperature for the processed polymer, the proper amount of material extrusion, and the correct printing speed directly affect the bonding of layers. The discontinuities in the parts cause them not to exhibit the expected properties. For example, the separation of the layers (delamination) and their inconsistency affect the part's mechanical properties.

In this study, specimen production was carried out using PET material with FFF technology. 3-point bending tests were carried out on the parts produced as ideal and artificially defected in different layer thicknesses. In addition, the separation of layers (delamination) methodology was developed with numerical analysis (Ansys).

2. MATERIALS AND METHODS

2.1. Materials

Ultrafuse PET product of BASF company was used in the study. This material is efficiently processed with the FFF method, 100% recyclable, waterproof and food-approved raw material. The PET filament used has a density of 1.329gr/cm3. Glass transition temperature (Tg) value is 71°C, and the melting Vol.ume rate is 16.3 cm3/10min.

Polytetrafluoroethylene (PTFE) film was used to create artificial layer separation defects (delamination) in the specimens produced by the FFF method using PET material. PTFE films are Aldrich brand, the product number is GF00775122, and the thickness is 10 microns.

2.2. Specimens Preparation

Specimens were prepared using PET filaments with the Ultimaker brand model 3 FFF device. All specimen productions were carried out with a single infill pattern; production was carried out in the -/+45 direction. The 3-point bending test specimens were produced by the ASTM D790-10 standard named Standard Test Methods for Flexural Properties of Unreinforced and Reinforced Plastics and Electrical Insulating Materials. The dimensions of the test specimens are as seen in figure 1. Drawings were made with the Fusion 360 program. The width and depth of the test specimens were drawn by the statement “Specimens with a depth of 3.2 mm or less should have a width of 12.7 mm”, specified in the standard.

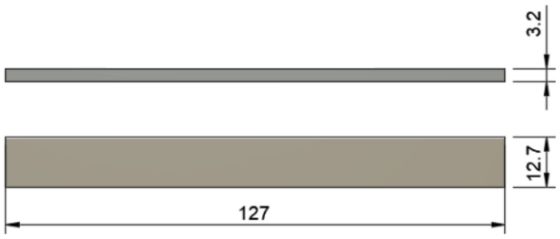

Figure 1. Dimensions of bending test specimens.

Specimens were produced in 3 different layer thicknesses (0.1/0.2/0.3mm). Production parameters are as seen in Table 1.

Bending test specimens produced in 3 different layer thicknesses consist of 2 groups of ideal and artificial defects. Six samples were produced for standard deviation calculations from all specimen varieties. The ideal bending test specimens were produced according to the dimensions in figure 1.

Table 1. FFF production parameters.

Parameters	Value
Nozzle diameter	400micron
Infill Density	100%
Printing Temperature	260°C
Build Plate Temperature	80°C
Material Flow	100%
Print Speed	300 mm/s
Cooling Fan Speed	10%
Support	None
Build Plate Adhesion	None

Specimens containing artificial defects (delamination) were produced by creating an artificial defect in the section shown in figure 2. The delamination width was calculated by the statement "The support span for all tests should be 16 times the beam depth" specified in the standard. PTFE film was placed on the layers indicated in Table 2 to create artificial defects in a controlled manner. During the production with FFF, the production was paused on the layers related to the code written with the CAM program (CURA), and the production continued after the PTFE application. The dimensions of the PTFE films placed in the middle layers are as seen in figure 2.7

Table 2. Number of the layer to locate delamination.

Specimens	Number of Total Layers	Number of the layers to located artificial defect
0.1 mm	32	16
0.2 mm	16	8
0.3 mm	10	5

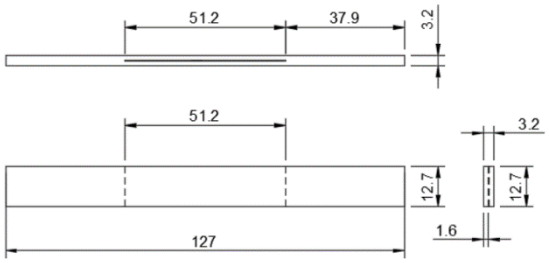

Figure 2. Area of artificial delamination.

Six delamination-free control specimens were produced for each layer thickness. Again, six pieces of each layer thickness were produced from the specimens containing artificial delamination in the layers specified in table 2 and the regions in figure 2 with three different layer thicknesses. The specimens produced are shown in Figure 3.

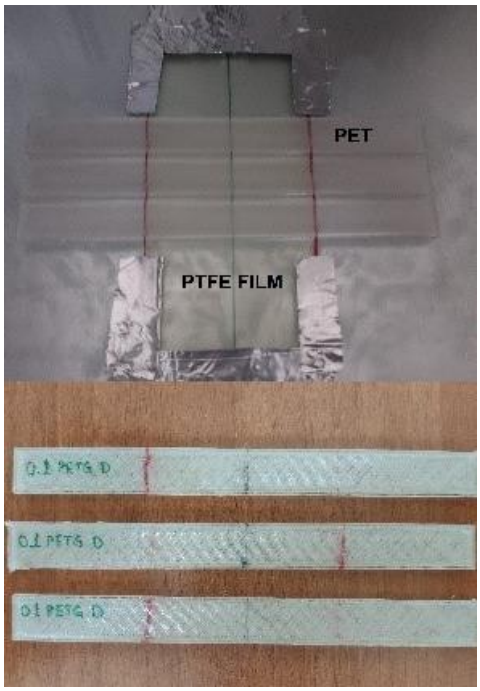

Figure 3. Specimens that included delamination.

2.2. Experimental Testing

A 3-point bending test was performed on the specimens produced by the FFF method using PET material. The 3-point bending tests were carried out by the ASTM D790-10 [27], standard named Standard Test Methods for Flexural Properties of Unreinforced and Reinforced Plastics and Electrical Insulating Materials. Figure 4 shows specimens tested. In addition, 3-point bending tests were performed on the Instron 1114 device shown in figure 5.

Figure 4. Experimental bending test specimens produced.

Figure 5. Bending test device.

As specified in the standard, the support span for all tests was placed at 16 times the beam depth.

When an elastic material is tested in bending as a simple beam with two points supported and force applied at the midpoint, the maximum stress on the outer surface of the test specimen occurs at the midpoint. This resulting stress can be calculated for any point on the load-deflection curve using equation 1.

$$\sigma_f = 3\,PL/\,2bd^2 \quad (1)$$

σ = stress in the outer fibres at the midpoint, MPa
P = load at a given point on the load-deflection curve, N
L = support span, mm
b = width of beam tested, mm
d = depth of beam tested, mm.

The bending moment at the midpoint of the beam surface is equal to the maximum stress. When the force reaches the load at the breaking moment, it is calculated from equation (1). No bending moment can be found if the material is not broken or completely damaged. If the materials do not break, it is necessary to find their yield strength. Stress is calculated by substituting the load in equation (1) for the place (yield point) entered in the plastic region in the load-deflection curve. This stress is the yield strength.

A maximum strain occurs at the lower surface of the beam, at the midpoint of the supports. The strain here is calculated by equation (2).

$$\epsilon_f = 6\,Dd/\,L^2 \quad (2)$$

ϵ_f = strain in the outer surface, mm/mm,
D = maximum deflection of the centre of the beam, mm,
L = support span, mm,
d = depth, mm.

2.3. Numerical Analyzing

The 3-point bending test was analysed numerically through the ANSYS program. Experimentally tested parts are modelled. For homogeneous PET materials, artificial delamination and ideal specimens were examined separately.

The properties of the PET material in the 'Granta Design Sample Materials' library in the ANSYS 19.2 program are given in Table 3.

Table 3. Properties of PET material in ANSYS 19.2

Property	Value	Unit
Density	1340	Kg m^-3
Young's Modulus	2.9E+09	Pa
Poisson's Ratio	0.389	
Bulk Modulus	4.3544E+09	Pa
Shear Modulus	1.0439E+09	Pa
Tensile Yield Strength	5.24E+07	Pa
Tensile Ultimate Strength	5.74E+07	Pa

The boundary conditions of the artificially delaminated and ideal specimens produced in

different layers were determined. Each layer is modelled as SHELL 181, and the layer thickness is given. SHELL181 is suitable for analysing thin to moderately thick shell structures. It is a four-node element with six degrees of freedom at each node: translations in the x, y, and z directions and rotations about the x, y, and z-axes. It was assumed that there is no adhesion in the delamination layer (PTFE included layer). A sticky and frictional surface was defined between the layers. The pressing head was moved for 11 mm with a speed of 1 mm/sec. Large deformation was accepted. Around 80000 nodes were used. Mesh quality is 93 per cent and above. Depending on the geometry, the force concentrations at the corners and sharp points were neglected.

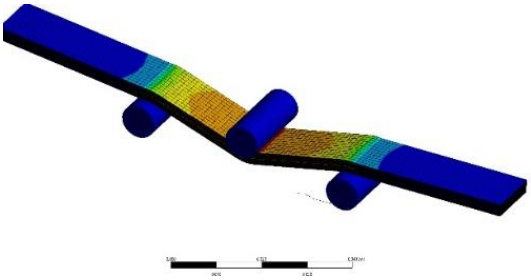

Figure 6. Finite element analysis.

3. RESULTS AND DISCUSSION

Figure 7 shows the average force and deflection graphs of PET specimens with and without delamination produced in 3 different layer thicknesses. In Figure 8, the numerical analysis results of the bending test of the PET test geometry with and without delamination in 3 different layer thicknesses are shared.

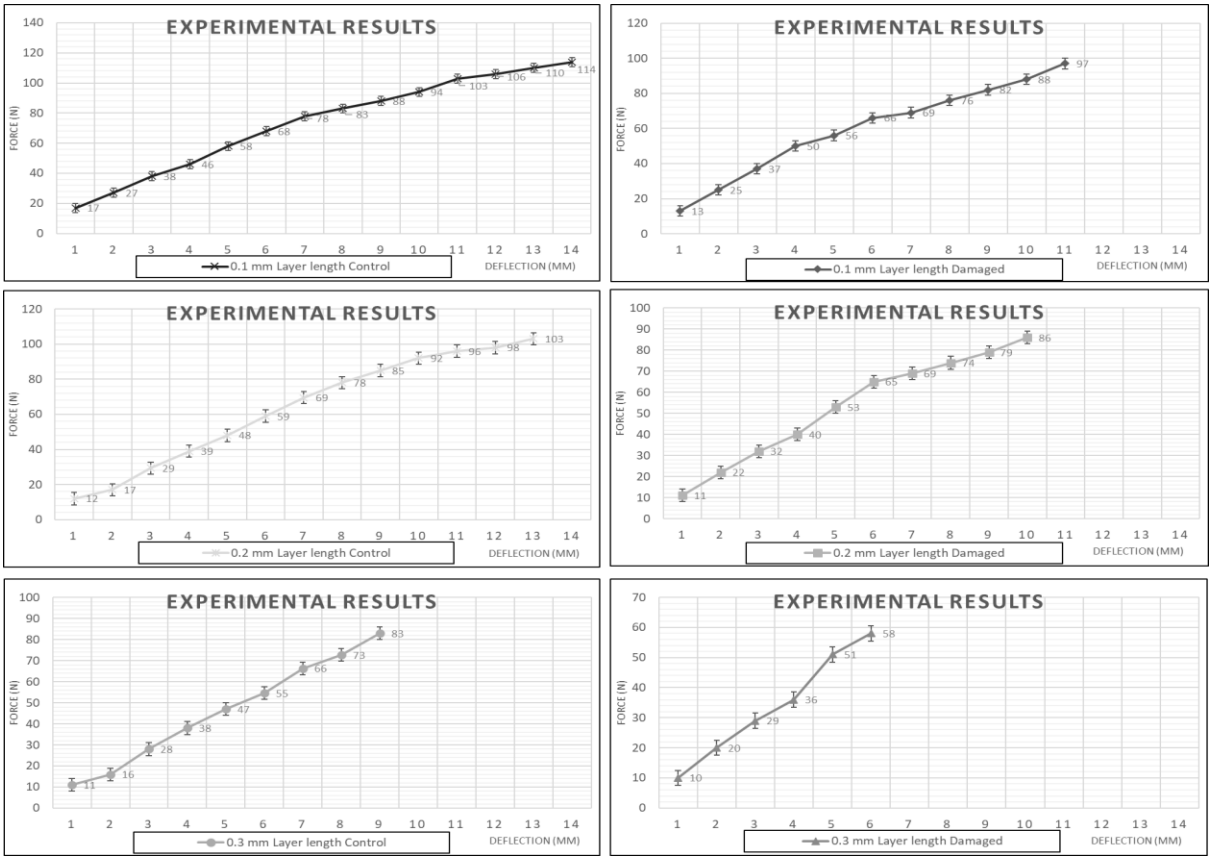

Figure 7. Experimental force-deflection graph.

The ideal specimens with a layer thickness of 0.1mm using PET material have the highest deflection and force. It performed a deflection of 14.25mm under a force of 114N. The specimens with a layer thickness of 0.1mm lost their stiffness after a further 114N force, and the force decreased. A 13mm deflection was observed under a force of 103N in the ideal specimens produced with a layer thickness of 0.2mm. After exceeding the 103N force, the specimens lost their stiffness like 0.1-layer specimens. Other specimens with 0.3mm layer thickness in the control group had a deflection of 9.71mm under 83N force and fractured.

The increase in layer thickness reduced the deflection under force. The specimens with a layer thickness of 0.3mm consisted of 10 layers. For this reason, it was fractured more easily than others. Specimens with 0.1 and 0.2mm layer thicknesses are formed by more layers, allowing deflection between the layers by shear stress. For this reason, the fracture did not occur in ideal specimens consisting of thinner and many layers.

The specimens produced in 0.1mm layer thickness containing delamination deflected 11.43mm under 97N force and fractured. The specimens produced with a layer thickness of 0.2mm that contained delamination had a deflection of 9.8mm under an average force of 86N and then cracked. The specimens produced with a layer thickness of 0.3mm that contained delamination, on the other hand, had a deflection of 5.98mm under an average force of 58N and then fractured. All specimens with delamination were cracked because of 3-point bending tests. This is an indication that layer separation has caused breakage.

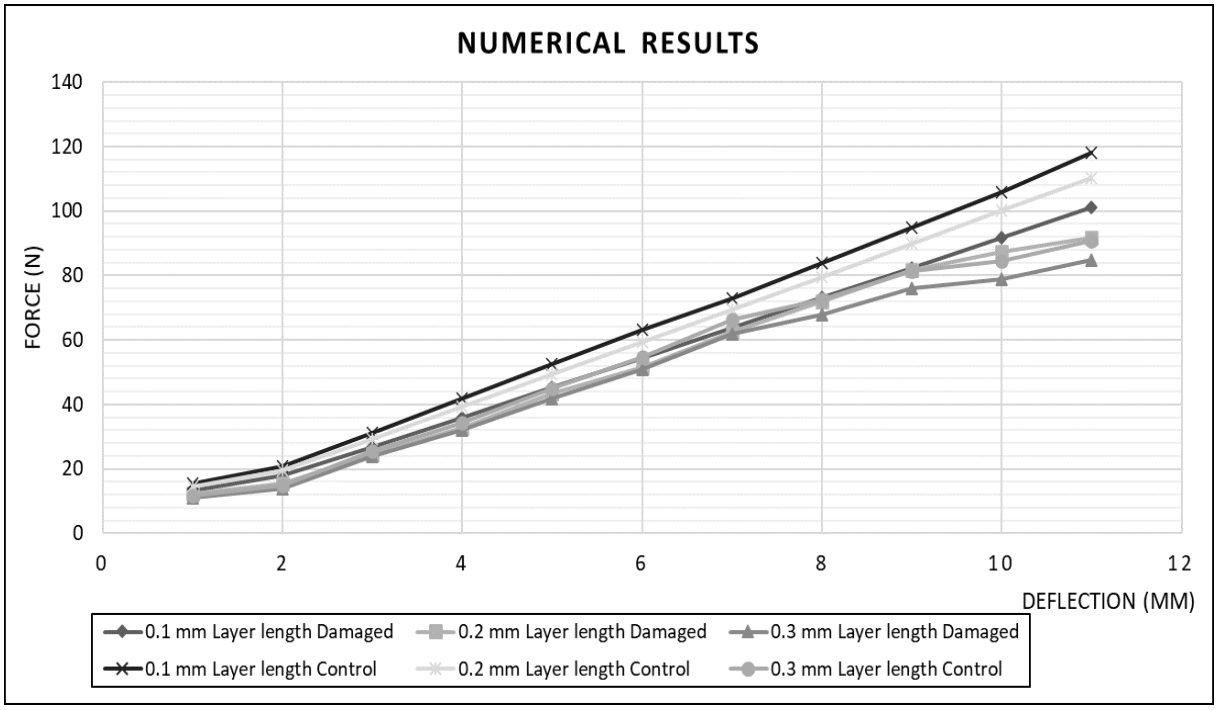

Figure 8. Numeric force-deflection graph.

Numeric analyses were carried out up to the maximum deflection value of 11mm, common to all control groups. The force values at which the ideal geometries in the control group performed a deflection of 11mm; were 118N at 0.1mm layer thickness, 110N at 0.2mm layer thickness, and 91N at 0.3mm layer thickness. These results show that as the layer thickness increases, the flexural strength decreases in numeric modelling.

The forces applied to the specimens containing delamination for 11mm deflection are, respectively, 101N with 0.1mm layer thickness, 92 with 0.2mm layer thickness, and 85N with 0.3mm layer thickness. Flexural strength was decreased by delamination in each specimen group. Experimental results and numerical analysis results confirm each other. Layer separation created as artificial delamination reduced the flexural strength as expected.

The stress values calculated by equation 1 and strain values calculated by equation 2 are given in Table 4. Experimental analysis results showed that the increase in the layer thickness of the specimens produced by the FFF method reduces the stress value at the midpoint of the beam. In addition, as the layer thickness increases, the strain also decreases. This is because the increase in layer thickness reduces the number of layers required to produce the geometry of the same thickness. Increasing the number of layers ensures that the geometry exhibits a more rigid stance.

Table 4. Bending stress and strain for experimental results.

Specimens	Stress (MPa)	Strain
0.1mm Layer Control	67.323	0.104
0.2mm Layer Control	60.827	0.095
0.3mm Layer Control	49.016	0.071
0.1mm Layer Damaged	57.283	0.084
0.2mm Layer Damaged	50.787	0.072
0.3mm Layer Damaged	34.252	0.044

When the specimens with and without delamination at the same layer thickness were compared, layer separation reduced the midpoint stress and strain. Flexural strength was reduced with delamination at 0.1mm layer thickness by 14.91%, at 0.2mm layer thickness by 16.5%, and at 0.3mm layer thickness by 30.12%. Ameri et al. [28], have shown that a stress riser, such as a hole in specimens produced with FFF, can reduce the loading capacity of the material by 17%. Delamination can also be characterised as a stress riser. The increase in layer thickness increased the acceleration of the decrease in flexural strength. Specimens with low layer thickness have more layers, reducing the effect of delamination.

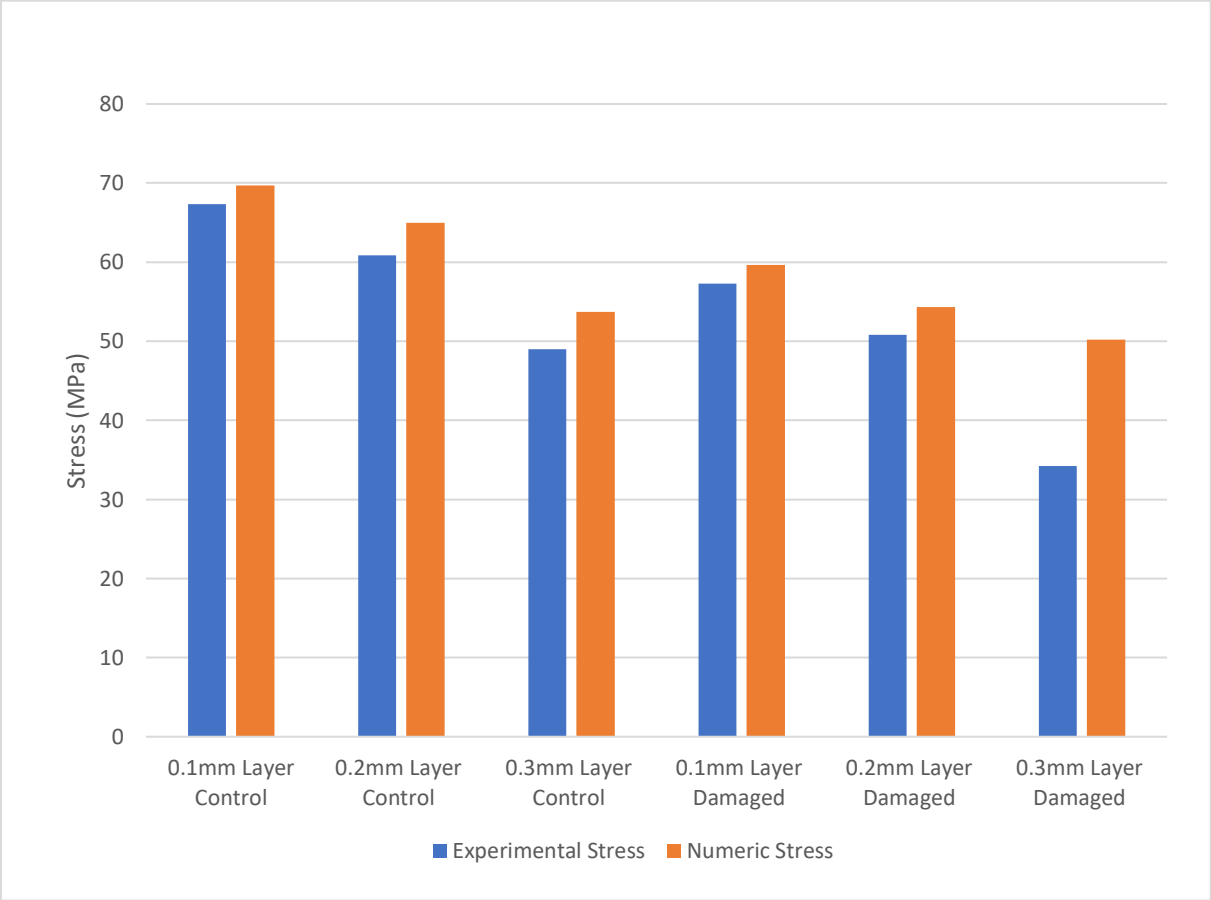

Figure 9. Flexural stress result.

Strain decreased with delamination at 0.1mm layer thickness by 19.23%, at 0.2mm layer thickness by 24.21%, and at 0.3mm layer thickness by 38.02%. Strain values, such as flexural stress values, decreased with increasing layer thickness. Although the increase in layer thickness makes the structure more rigid, delamination caused a more significant reduction in the strain at higher layer thickness.

Table 5. Flexural Stress for Numeric Results

Specimens	Stress (MPa)
0.1mm Layer Control	69.69
0.2mm Layer Control	64.96
0.3mm Layer Control	53.74
0.1mm Layer Damaged	59.65
0.2mm Layer Damaged	54.33
0.3mm Layer Damaged	50.2

The numeric analysis showed that the increase in the layer thickness decreases the flexural strength. It has also been calculated that

delamination, as seen in figure 10, reduces the flexural strength at the relevant layer thickness. Damage mechanics are pretty complicated. While fluctuations appear in experimental results, a linear curve is generally seen in numerical results. In addition, numeric results were higher. The main reason for this is the micro-level gaps and production failures in additive manufacturing.

Figure 10. Plastic delamination.

4. CONCLUSIONS

Perfect production is the most fundamental component of the concept of quality. In this understanding, zero-defect reduces costs. Nozzle clogging, non-adhesion of the first layer, incomplete extruding of the material, production deformation (warping) of the part, failure of the layers to bonding, etc., are the main problems encountered in the FFF method. These defects cause the manufactured parts not to exhibit the expected properties. It is also known that the parts produced by the FFF method have anisotropic properties. The z-axis is the axis in which the parts produced with the FFF exhibit the lowest mechanical properties. Since the part is extruded in layers due to the nature of FFF production technology, it is critical for the strength of the part that the layers are interconnected and create strength in the z-direction. This study showed that delamination in a specimen produced with FFF could reduce flexural strength by 30%. Numeric analyses performed were confirmed by experimental tests. As a result of the tests and examinations, it was determined that the increase in the layer thickness decreases the flexural strength and strain value.

In FFF technology, damage that may occur in a single layer can weaken the entire structure by more than 10%, depending on the layer thickness. This shows that production quality is critical for FFF technology. For future studies, more precise results can be obtained if a model with micro-level damage mechanics is made by considering the product gaps in additive manufacturing.

REFERENCES

1. Szczepanik, S. and Bednarczyk, P., “Bending and Compression Properties of ABS and PET Structural Materials Printed Using FDM Technology”, J. Cast. Mater. Eng., Vol. 1, Issue 39, 2017.

2. Exconde, E., Co, A., Manapat, Z. and Magdaluyo, R., “Materials selection of 3D printing filament and utilization of recycled polyethylene terephthalate (PET) in a redesigned breadboard”, Procedia CIRP, Issue 84, Pages 28-32, 2019.

3. Nisticò, R., “Polyethylene terephthalate (PET) in the packaging industry”, Polym. Test., Vol. 90, Issue 106707, 2020.

4. Latko-Durałek, P., Dydek, K. and Boczkowska, A., “Thermal, Rheological and Mechanical Properties of PETG/rPETG Blends”, J. Polym. Environ., Vol. 27, Pages 2600–2606, 2019.

5. Sarkar, K. , “Polyester derived from recycled polyethylene terephthalate waste for regenerative medicine”, RSC Adv., Vol. 4, Pages 58805–58815, 2014.

6. Shamsi, R., Mir, M. and Sadeghi, G., “Novel polyester diol obtained from PET waste and its application in the synthesis of polyurethane and carbon nanotube-based composites: swelling behavior and characteristic properties”, RSC Adv., Vol. 6, Pages 38399–38415, 2016.

7. Nadkarni, V. M., Shingankuli, V. L., and Jog, J. P., “Effect of blending on the crystallization behavior of PET”, J. Appl. Polym. Sci., Vol. 46, Pages 339-351, 1992.

8. Reis, J. M. L., Chianelli-Junior, R., Cardoso, J. L. and Marinho, F. J. V., “Effect of recycled PET in the fracture mechanics of polymer mortar”, Constr. Build. Mater., Vol. 25, Pages 2799–2804, 2011.

9. Malik, N., Kumar, P., Shrivastava, S. and Ghosh, S. B., “An overview on PET waste recycling for application in packaging”, Int. J. Plast. Technol., Vol. 211, Issue 21, Pages 1–24, 2016.

10. Chen, T., Zhang, J. and You, H., “Photodegradation behavior and mechanism of poly(ethylene glycol-co-1,4-cyclohexanedimethanol terephthalate) (PETG) random copolymers: correlation with copolymer composition”, RSC Adv., Vol. 6, Pages 102778–102790, 2016.

11. Wang, X., et al., "Study on the effect of dispersion phase morphology on porous structure of poly (lactic acid)/poly (ethylene terephthalate glycol-modified) blending foams", Polymer (Guildf)., Vol. 54, Pages 5839–5851, 2013.

12. Kumar, M. A., Khan, M. S. and Mishra, S. B., "Effect of machine parameters on strength and hardness of FDM printed carbon fiber reinforced PETG thermoplastics", Mater. Today Proc., Vol. 27, Pages 975–983, 2019.

13. Sood, A. K., Ohdar, R. K. and Mahapatra, S. S., "Parametric appraisal of mechanical property of fused deposition modelling processed parts", Mater. Des., Vol. 31, Pages 287–295, 2010.

14. Srinivasan, R., Prathap, P., Raj, A., Kannan, S. A. and Deepak, V., "Influence of fused deposition modeling process parameters on the mechanical properties of PETG parts", in Materials Today: Proceedings, Vol. 27, Pages 1877–1883, 2020.

15. Durgashyam, K., Reddy Indrra, M., Balakrishna, A. and Satyanarayana, K., "Experimental investigation on mechanical properties of PETG material processed by fused deposition modeling method", in 2nd International Conference on Applied Sciences and Technology (ICAST-2019): Materials Science, Pages 2052–2059, 2019.

16. Sepahi, M. T., Abusalma, H., Jovanovic, V. and Eisazadeh, H., "Mechanical Properties of 3D-Printed Parts Made of Polyethylene Terephthalate Glycol", J. Mater. Eng. Perform., Vol. 30, Pages 6851–6861, 2021.

17. Hanon, M. M., Marczis, R. & Zsidai, L. "Anisotropy Evaluation of Different Raster Directions, Spatial Orientations, and Fill Percentage of 3D Printed PETG Tensile Test Specimens", Key Eng. Mater., Vol. 821, Pages 167–173, 2019.

18. Mansour, M., Tsongas, K., Tzetzis, D. and Antoniadis, A., "Mechanical and Dynamic Behavior of Fused Filament Fabrication 3D Printed Polyethylene Terephthalate Glycol Reinforced with Carbon Fibers", Polym. - Plast. Technol. Eng., Vol. 57, Pages 1715–1725, 2018.

19. Fonseca, J., Ferreira, I. A., de Moura, M. F. S. F., Machado, M. and Alves, J. L. "Study of the interlaminar fracture under mode I loading on FFF printed parts", Compos. Struct., Vol. 214, Pages 316–324, 2019.

20. Atlıhan, G., Ovalı, İ. and Eren, A. "Eklemeli İmalat Yöntemiyle Üretilmiş Bal Petekli Yapıların Titreşim Davranişlarının Nümerik ve Deneysel Olarak İncelenmesi", Int. J. 3D Print. Technol. Digit. Ind., Vol. 5, Pages 98-108, 2021.

21. Somireddy, M., Singh, C. V. and Czekanski, "A. Analysis of the Material Behavior of 3D Printed Laminates Via FFF", Exp. Mech., Vol. 59, Pages 871–881, 2019.

22. Yao, T., Ouyang, H., Dai, S., Deng, Z. and Zhang, K. "Effects of manufacturing micro-structure on vibration of FFF 3D printing plates: Material characterisation, numerical analysis and experimental study", Compos. Struct., Vol. 268, Issue 113970, 2021.

23. García Plaza, E., Núñez López, P. J., Caminero Torija, M. Á. and Chacón M., J. M., "Analysis of PLA geometric properties processed by FFF additive manufacturing: Effects of process parameters and plate-extruder precision motion", Polymers (Basel)., Vol. 11, 2019.

24. Mazzanti, V., Malagutti, L. and Mollica, F. "FDM 3D printing of polymers containing natural fillers: A review of their mechanical properties", Polymers (Basel)., Vol. 11, 2019.

25. Bhandari, S. and Lopez-Anido, R. "Finite element analysis of thermoplastic polymer extrusion 3D printed material for mechanical property prediction", Addit. Manuf., Vol. 22, Pages 187–196, 2018.

26. Bellini, A. "Mechanical characterization of parts fabricated using fused deposition modeling", Rapid Prototyp. J., Vol. 9, Pages 252–264, 2003.

27. ASTM. D790 − 10 "StandardTest Methods for Flexural Properties of Unreinforced and Reinforced Plastics and Electrical Insulating Materials", http://www.ansi.org. doi:10.1520/D0790-10.

28. Ameri, B., Taheri-Behrooz, F. and Aliha, M. R. M. "Evaluation of the geometrical discontinuity effect on mixed-mode I/II fracture load of FDM 3D-printed parts", Theor. Appl. Fract. Mech., Vol. 113, Issue 102953, 2021.